Supporting Information

Non-Pinned, Reversible Spin Crossover in Self-Assembled Monolayers of a Functionalised Fe(II) Scorpionate Complex

Rebecca Rodrigues de Miranda, Niccolò Giaconi, Margaux Pénicaud, Lisa Biwandu, Thierry Buffeteau, Brunetto Cortigiani, Matteo Mannini, Edwige Otero, Philippe Ohresser, Elizabeth Hillard, Lorenzo Poggini, Mathieu Gonidec,* Patrick Rosa**

Figure S1

Vibrating Sample Magnetometry (VSM) magnetic measurement on bulk **FeTp$_2$-C11-SAc** in the warming mode (red triangles) and the cooling mode (blue triangles). The green curve represents the Boltzmann equilibrium fitting of the warming mode.

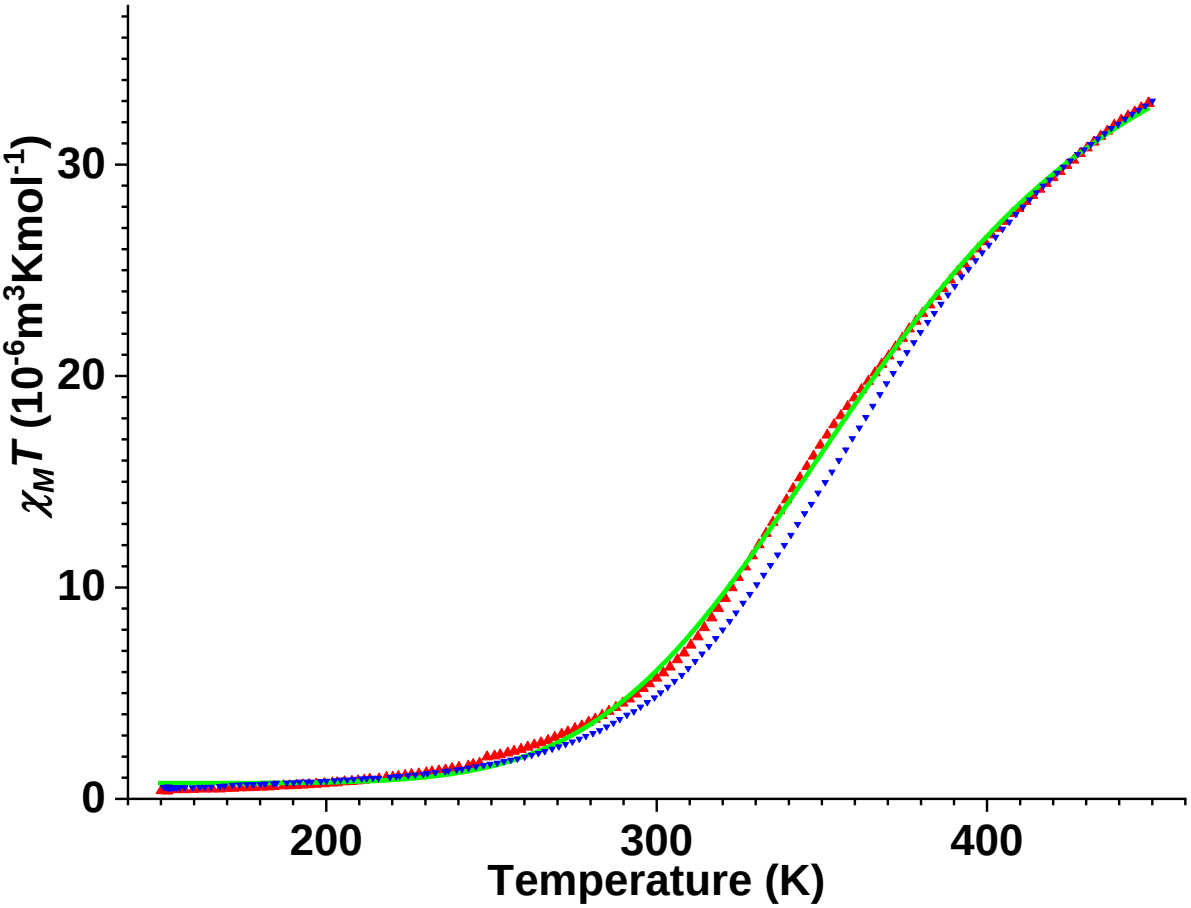

The raw magnetic data was converted to the molar susceptibility product with temperature, $\chi_M T$, after removing the sample holder magnetic background and sample diamagnetic contribution, estimated using Pascal's constants.

Below 200 K, $\chi_M T$ is very close to zero at 5×10^{-7} m^3 K mol^{-1}, in agreement with an essentially diamagnetic state. $\chi_M T$ increases monotonically with temperature above 250 K, to reach 33.0×10^{-6} m^3 K mol^{-1} at 450 K. This value is lower than the spin-only value of 37.7×10^{-6} m^3 K mol^{-1} expected for a HS Fe(II) complex with S = 2 and a g value of 2.0, but as can be seen the crossover is not complete at this temperature. A change in the curve slope is observed around 335 K, indicating some change in the complex, which we link to its melting within the sample holder. Accordingly, the measurement in the cooling mode does not fully follow the curve. Subsequent measurements stay close to both curves. We fitted the warming mode measurement considering a Boltzmann equilibrium between the two states (R^2 of 0.99949):

$$\chi_M T = \frac{\chi_M T_{max}}{1 + exp\left(\Delta H/_{RT} + \Delta S/_{R}\right)} + residue$$

We obtained a value of $39.1(1)\times10^{-6}$ m^3 K mol^{-1} for $\chi_M T_{max}$, a value slightly above the spin-only value for HS Fe(II). ΔH and ΔS values of 25.1(1) kJ mol^{-1} and 68.4(3) J K^{-1} mol^{-1} are in

agreement with a non-cooperative SCO with a $T_{1/2}$ of 367 K. The residue of 7.4(1) $\times 10^{-7}$ m^3 K mol^{-1} shows an almost complete SCO to the diamagnetic state. We used the value of $\chi_M T_{max}$ obtained by the fit to calculate the HS fraction n_{HS} reported in the main text.

Figure S2

AFM height map (top) of a bare template stripped gold substrate (left) and of a SAM of **FeTp$_2$-C11-S** on template stripped gold (right), on a 5 × 5 µm area. The SAM is uniform and marginally rougher than the bare gold, with a RMS roughness of 7.1 Å compared to 6.9 Å for the substrate. The corresponding phase images (bottom) are clearly distinct for the bare substrate (left) and the SAM (right).

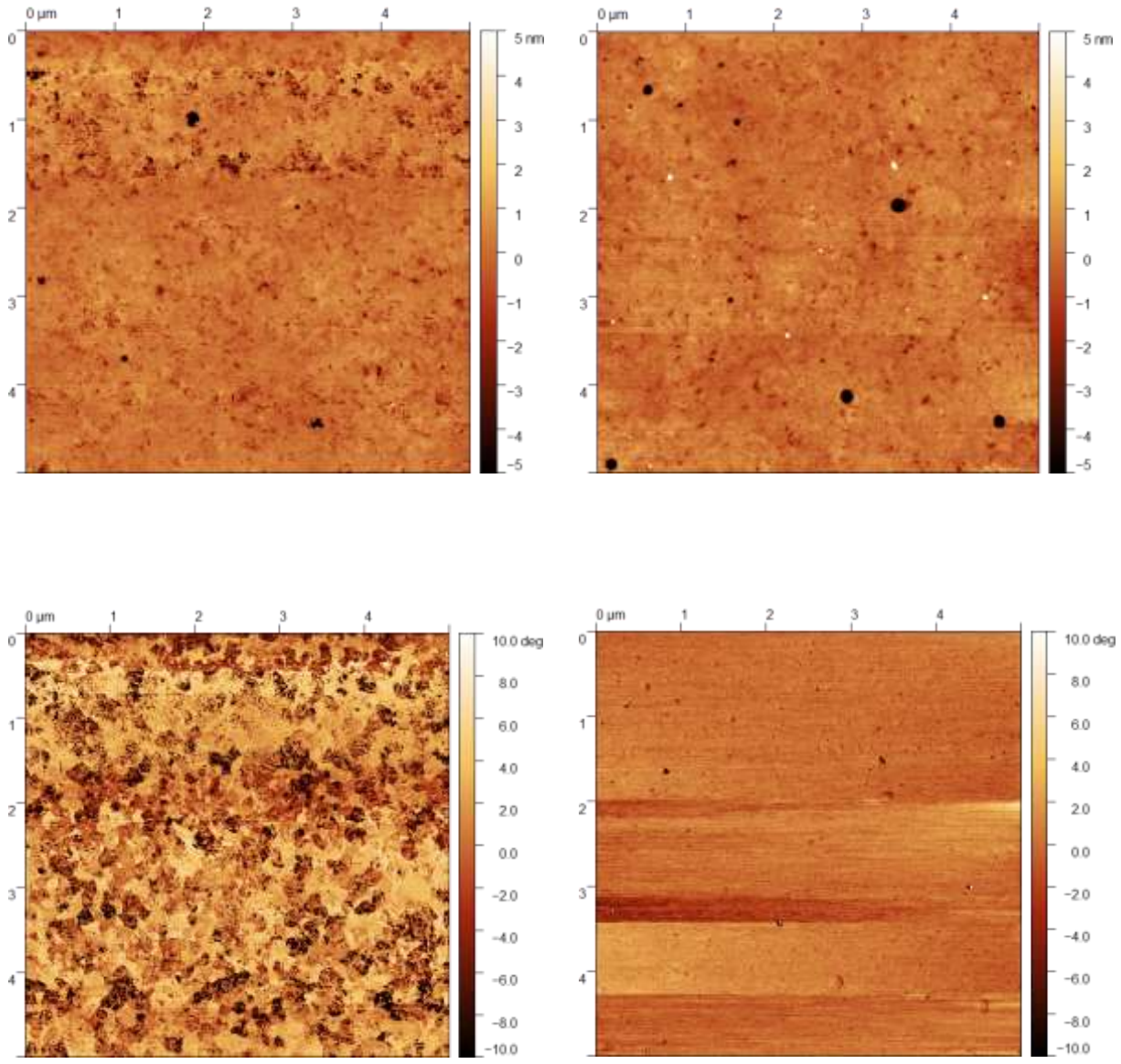

Figure S3

Time of Flight Secondary Ion Mass Spectrometry (ToF-SIMS) secondary ion mapping on a 500 × 500 µm area (top), confirming the presence of **FeTp$_2$-C11-S** on the Au^{TS}, as well as two molecular fragments presumably originating from fragmentation during measurement. The molecule and its fragments are homogeneously distributed over the imaged area. The isotopic distributions (bottom) correspond to the calculated patterns.

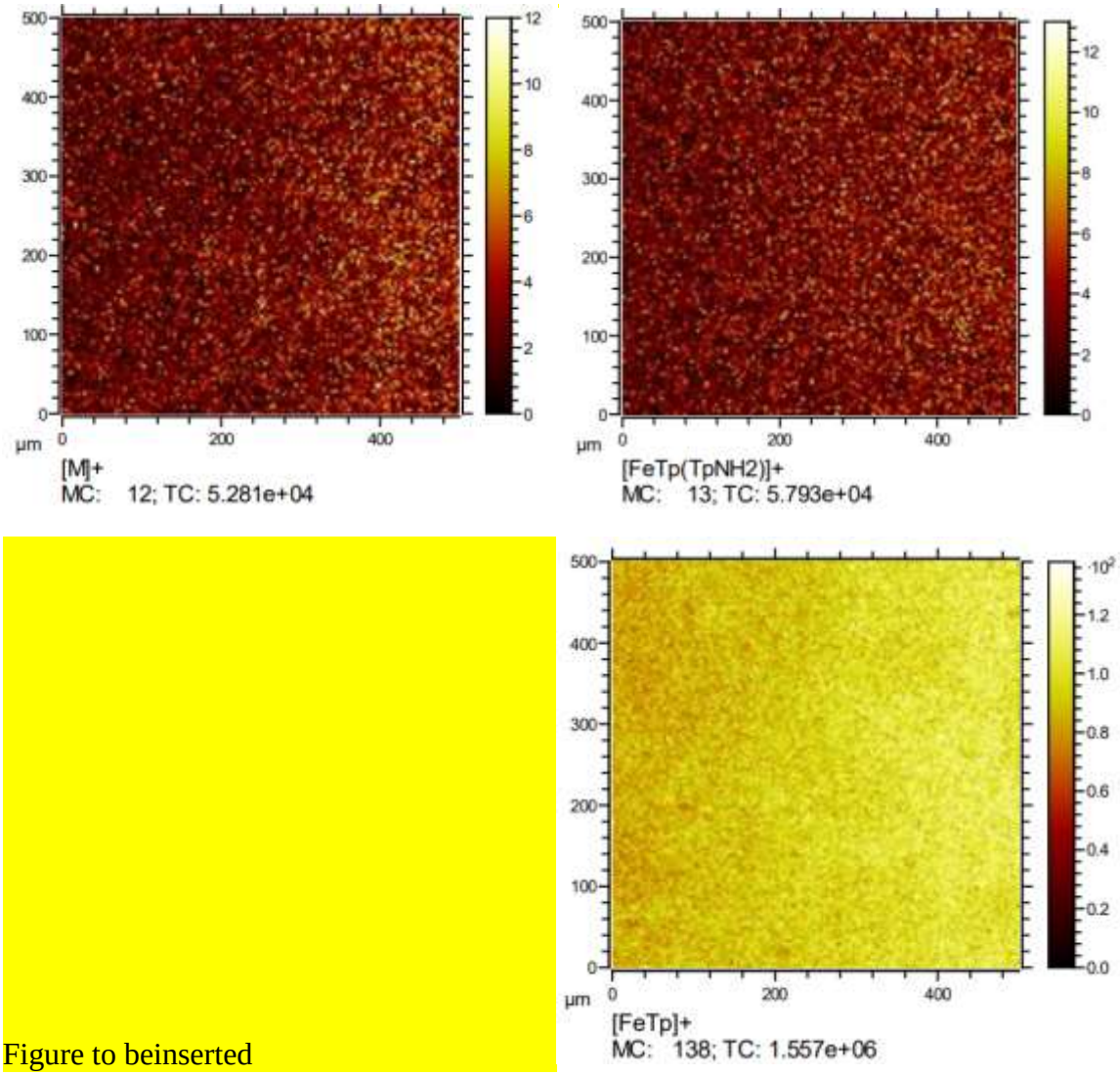

Figure to beinserted

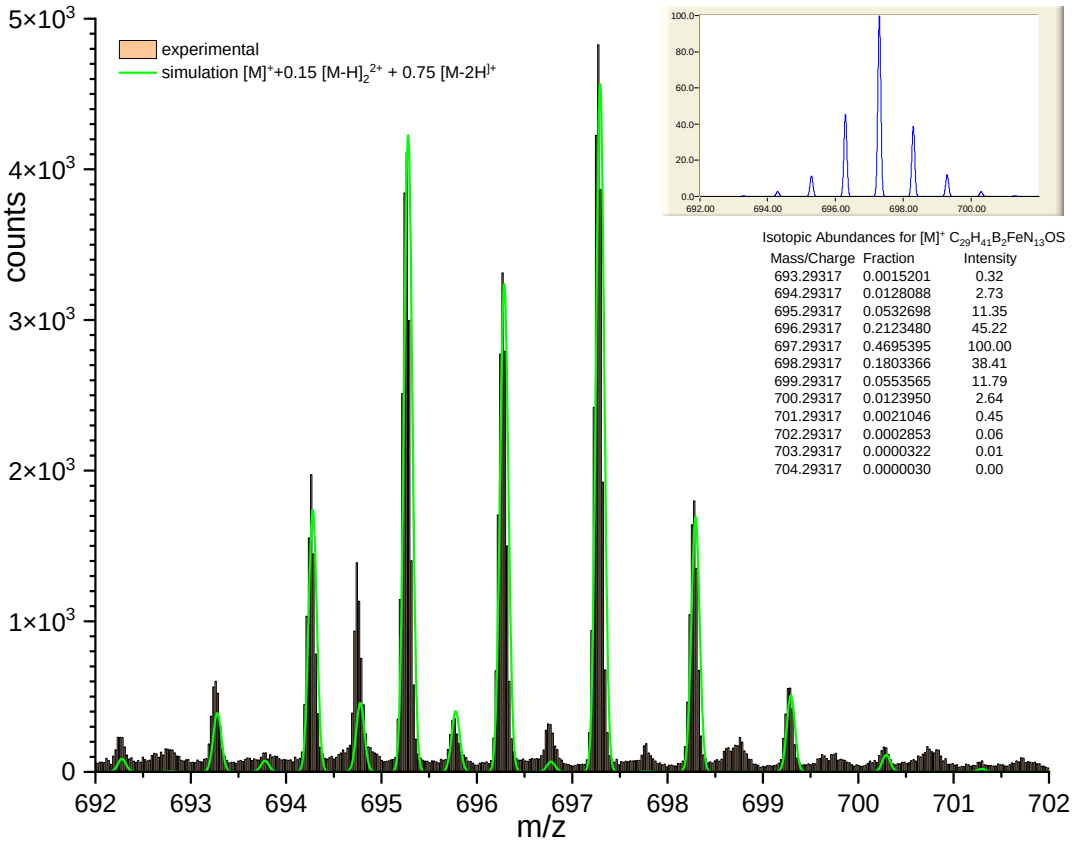

Isotopic Abundances for $[M]^+$ $C_{29}H_{41}B_2FeN_{13}OS$

Mass/Charge	Fraction	Intensity
693.29317	0.0015201	0.32
694.29317	0.0128088	2.73
695.29317	0.0532698	11.35
696.29317	0.2123480	45.22
697.29317	0.4695395	100.00
698.29317	0.1803366	38.41
699.29317	0.0553565	11.79
700.29317	0.0123950	2.64
701.29317	0.0021046	0.45
702.29317	0.0002853	0.06
703.29317	0.0000322	0.01
704.29317	0.0000030	0.00

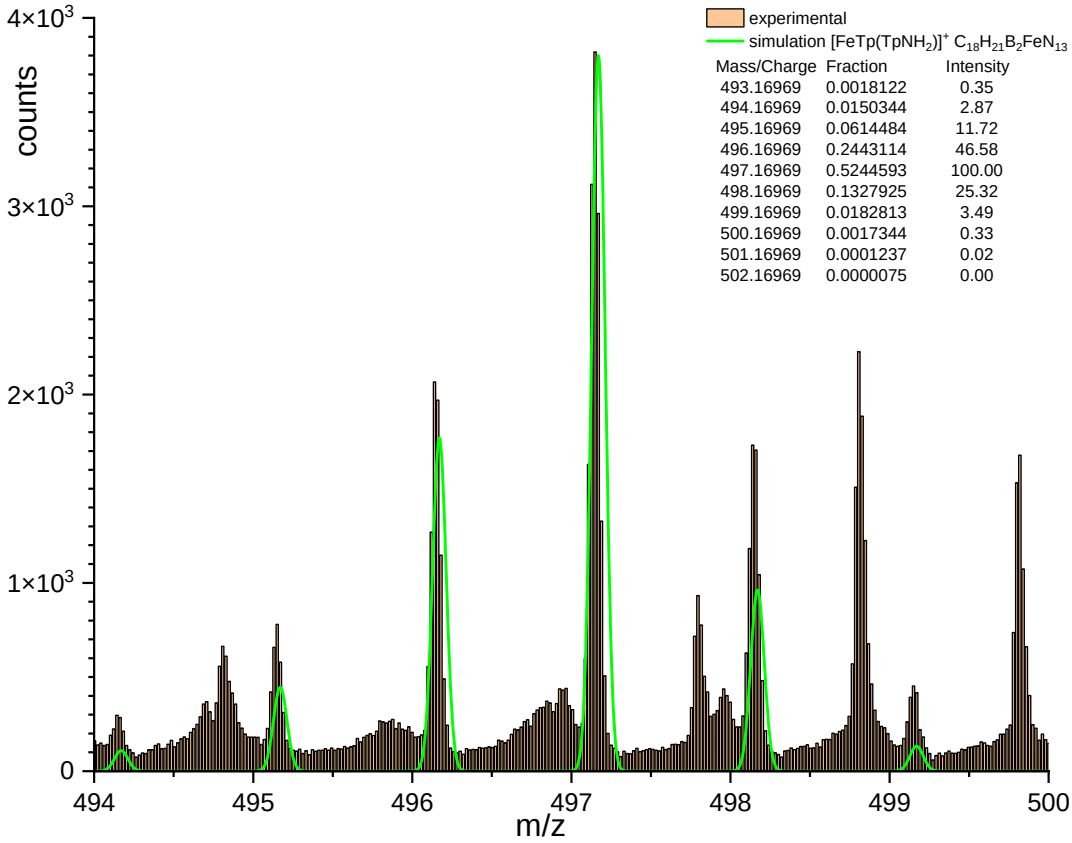

Mass/Charge	Fraction	Intensity
493.16969	0.0018122	0.35
494.16969	0.0150344	2.87
495.16969	0.0614484	11.72
496.16969	0.2443114	46.58
497.16969	0.5244593	100.00
498.16969	0.1327925	25.32
499.16969	0.0182813	3.49
500.16969	0.0017344	0.33
501.16969	0.0001237	0.02
502.16969	0.0000075	0.00

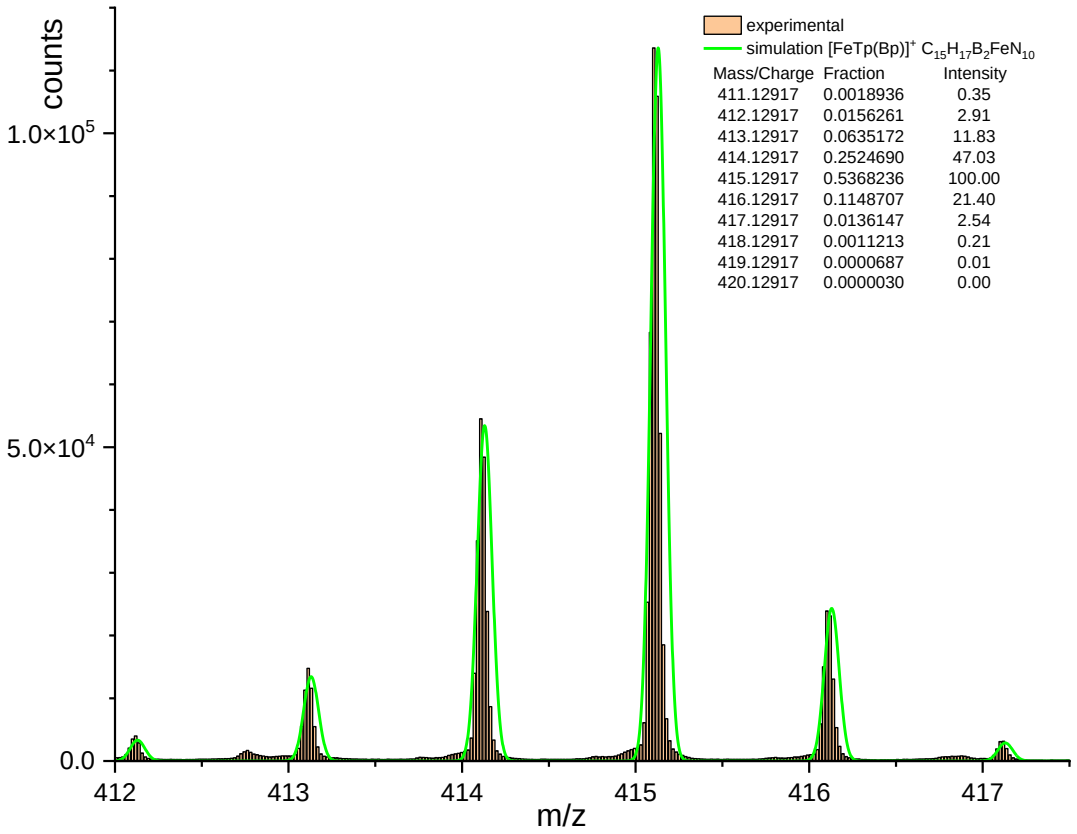
experimental
simulation [FeTp(Bp)]+ C15H17B2FeN10
Mass/Charge Fraction Intensity
411.12917 0.0018936 0.35
412.12917 0.0156261 2.91
413.12917 0.0635172 11.83
414.12917 0.2524690 47.03
415.12917 0.5368236 100.00
416.12917 0.1148707 21.40
417.12917 0.0136147 2.54
418.12917 0.0011213 0.21
419.12917 0.0000687 0.01
420.12917 0.0000030 0.00
counts
1.0×10^5
5.0×10^4
0.0
412
413
414
415
416
417
m/z

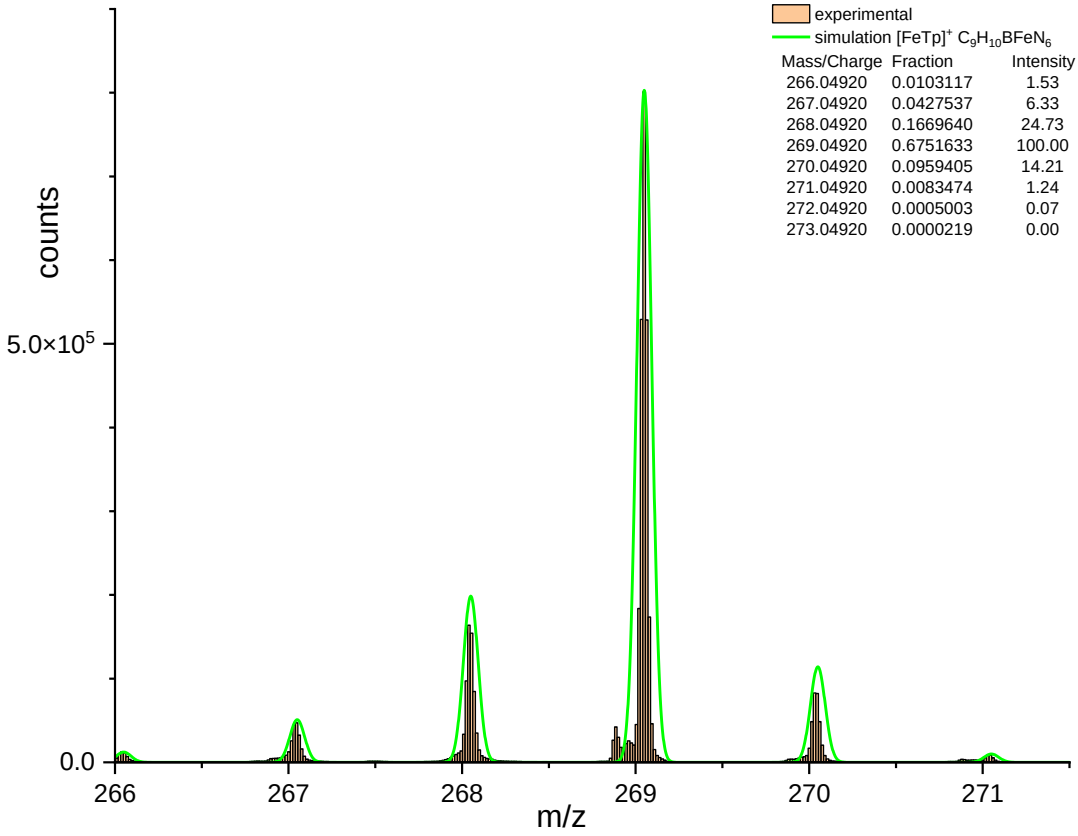
experimental
simulation [FeTp]+ C9H10BFeN6
Mass/Charge Fraction Intensity
266.04920 0.0103117 1.53
267.04920 0.0427537 6.33
268.04920 0.1669640 24.73
269.04920 0.6751633 100.00
270.04920 0.0959405 14.21
271.04920 0.0083474 1.24
272.04920 0.0005003 0.07
273.04920 0.0000219 0.00
counts
5.0×10^5
0.0
266
267
268
269
270
271
m/z

Figure S4

Room temperature X-ray Photoelectron Spectroscopy (XPS) on a SAM of **FeTp$_2$-C11-S** on gold, in the regions of the Fe*2p*, N*1s* and S*2p* binding energies. The measured data is plotted as open circles, with the solid red lines corresponding to the envelopes of the fitted components. The fitted components are represented with orange, blue and green solid lines. The spectra were fit in CasaXPS after calibrating to the Fermi value of the gold substrate and removing a step-like background. Calculated cross sections[1] were used and the peaks were fit with 70/30 Voigt functions.

The N*1s* peak is unchanged from the bulk, and can be fit with a single component. The S*2p* peak, however, is shifted to a lower binding energy in the SAM, confirming that the sulphur groups are anchored to the gold. Moreover, the peak is now split into two. As discussed in the main text, this comes from a certain amount of physisorbed sulphur, which has a different photoelectron binding energy from the chemisorbed sulphur.

Semi-quantitative analysis gives elemental ratios of Fe (7.4 ± 0.4%, theoretical 6.7%), N (82.6 ± 4.1%, theoretical 86.7%) and S (10.0 ± 0.5%, theoretical 6.7%) that correspond to the theoretical composition, considering the experimental error of the XPS. There is a slight excess of sulphur.

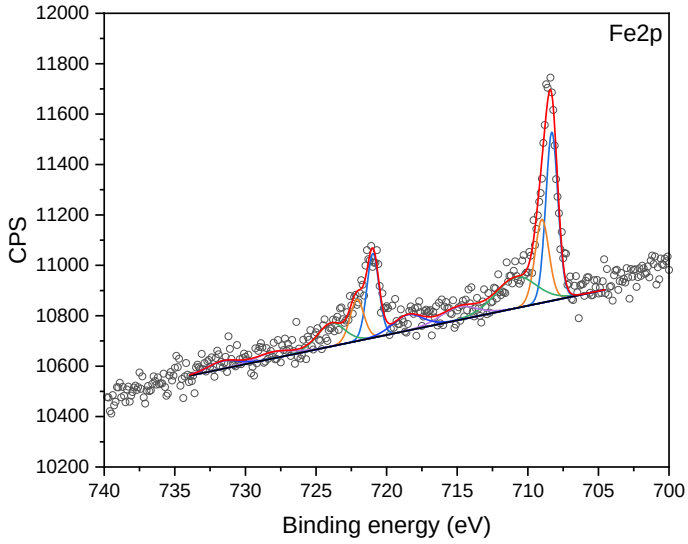
Fe2p
CPS
Binding energy (eV)
12000
11800
11600
11400
11200
11000
10800
10600
10400
10200
740
735
730
725
720
715
710
705
700

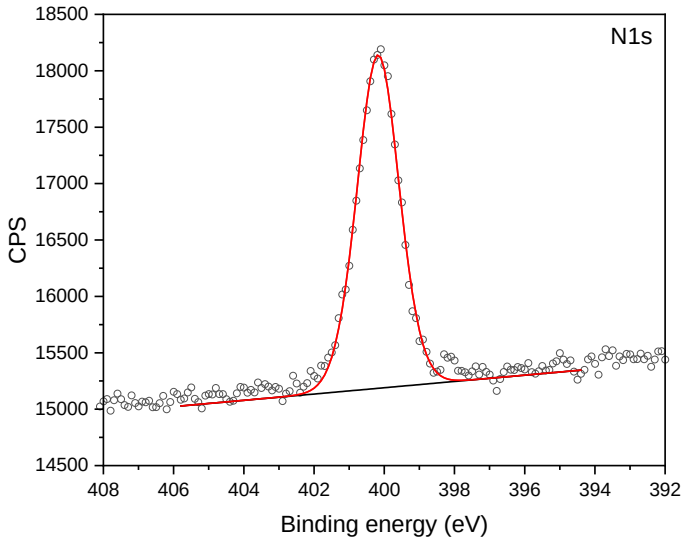
N1s
CPS
Binding energy (eV)
18500
18000
17500
17000
16500
16000
15500
15000
14500
408
406
404
402
400
398
396
394
392

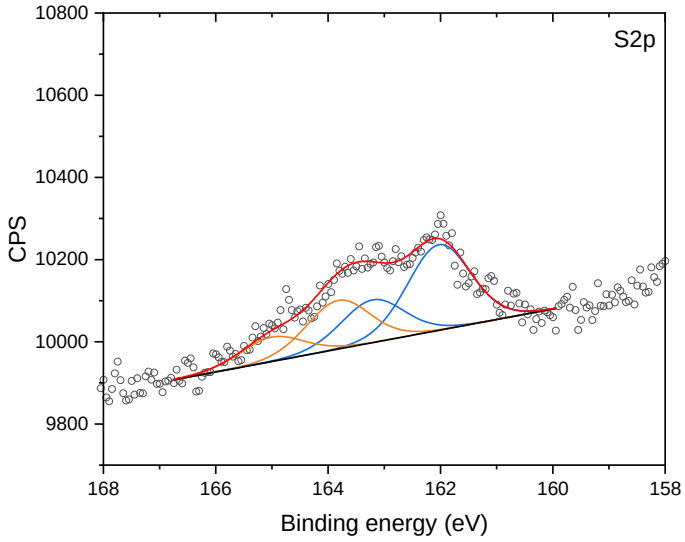
S2p
CPS
10800
10600
10400
10200
10000
9800
168
166
164
162
160
158
Binding energy (eV)

Figure S5a

Comparison of experimental IRRAS spectrum (in black) of an **FeTp$_2$-C11-S** SAM on Au^{TS} and simulated IRRAS spectra for **FeTp$_2$-C11-SAc** layers of various thicknesses (15 Å in red, 20 Å in blue and 25 Å in green).

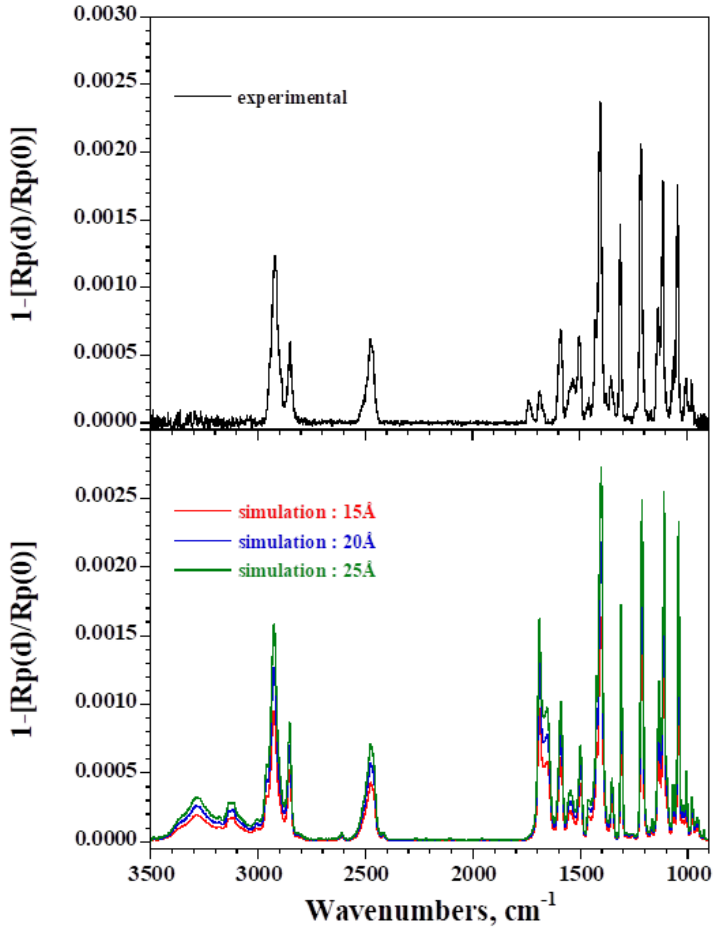

The isotropic and anisotropic optical constants (refractive index $n(\bar{\nu})$ and extinction coefficient $k(\bar{\nu})$) of **FeTp$_2$-C11-Sac**, have been determined from polarized ATR spectra (shown in **Figure S5b**), using the procedure described by Dignam *et. al.*.[2] Isotropic optical constants (*i.e.* similar values of the in-plane and out-of-plane refractive indexes and extinction coefficients) have been measured for **FeTp$_2$-C11-SAc** (**Figures S5c and S5d**). We have checked for this compound that the intensities of the bands in the p-polarized ATR spectrum are the double those measured in the s-polarized ATR spectrum, as is expected for an isotropic layer. The refractive index in the visible was set to 1.5 for **FeTp$_2$-C11-SAc**.

The program used to calculate the IRRAS spectra for a compact monolayer of **FeTp$_2$-C11-SAc** deposited onto gold substrate is based on the Abeles' matrix formalism,[3,4] which has been generalized for anisotropic layers.[5] Several parameters must be fixed in the program, such as the thickness of the monolayer, the angle of incidence (set to 75°) and the polarization of the infrared beam. The p-polarized reflectance of the covered $R_p(d)$ and bare $R_p(0)$ substrates have been calculated using the spectral dependence of the optical constants of **FeTp$_2$-C11-SAc** and of gold.[6]

Figure S5b

P-polarized and s-polarized ATR spectra of **FeTp$_2$-C11-SAc** film drop cast onto a Ge crystal.

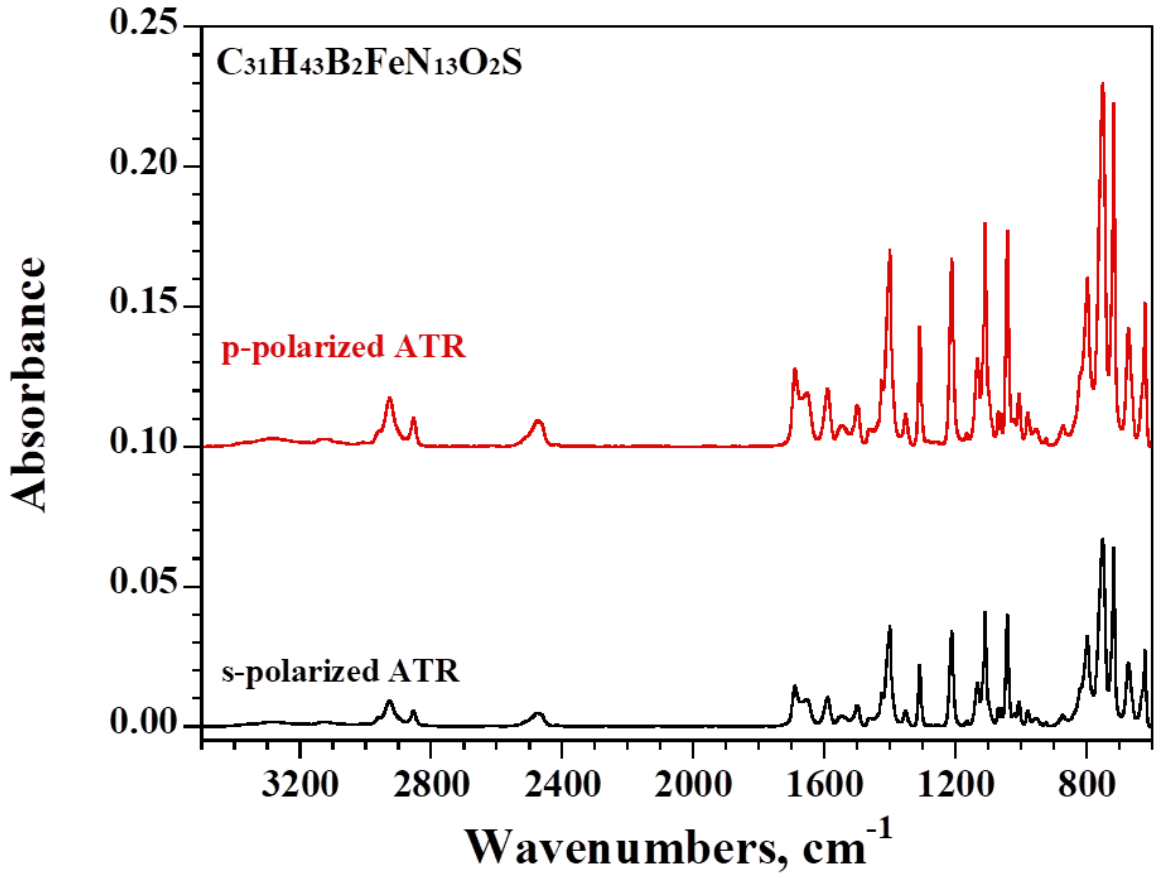

Figure S5c

Isotropic optical constants of **FeTp$_2$-C11-SAc**.

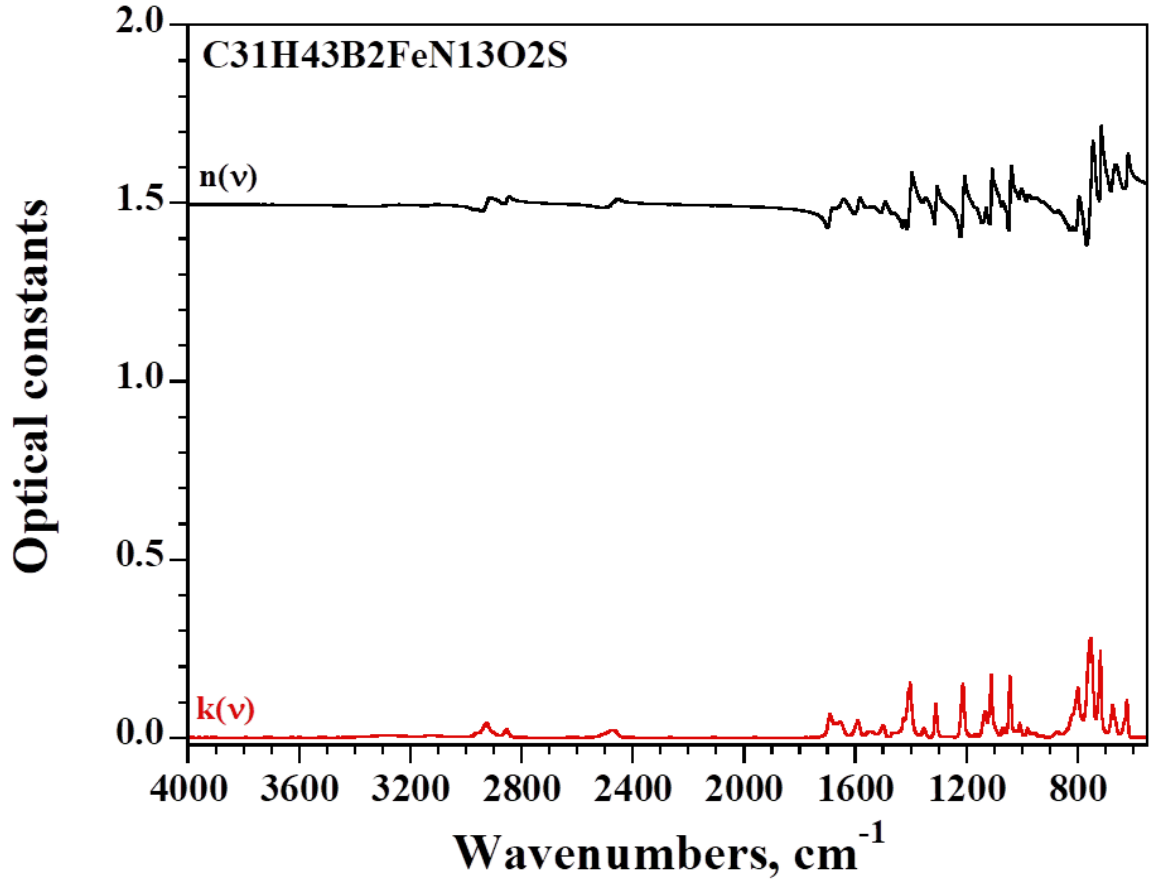

Figure S5d

Ansotropic optical constants of **FeTp$_2$-C11-SAc**.

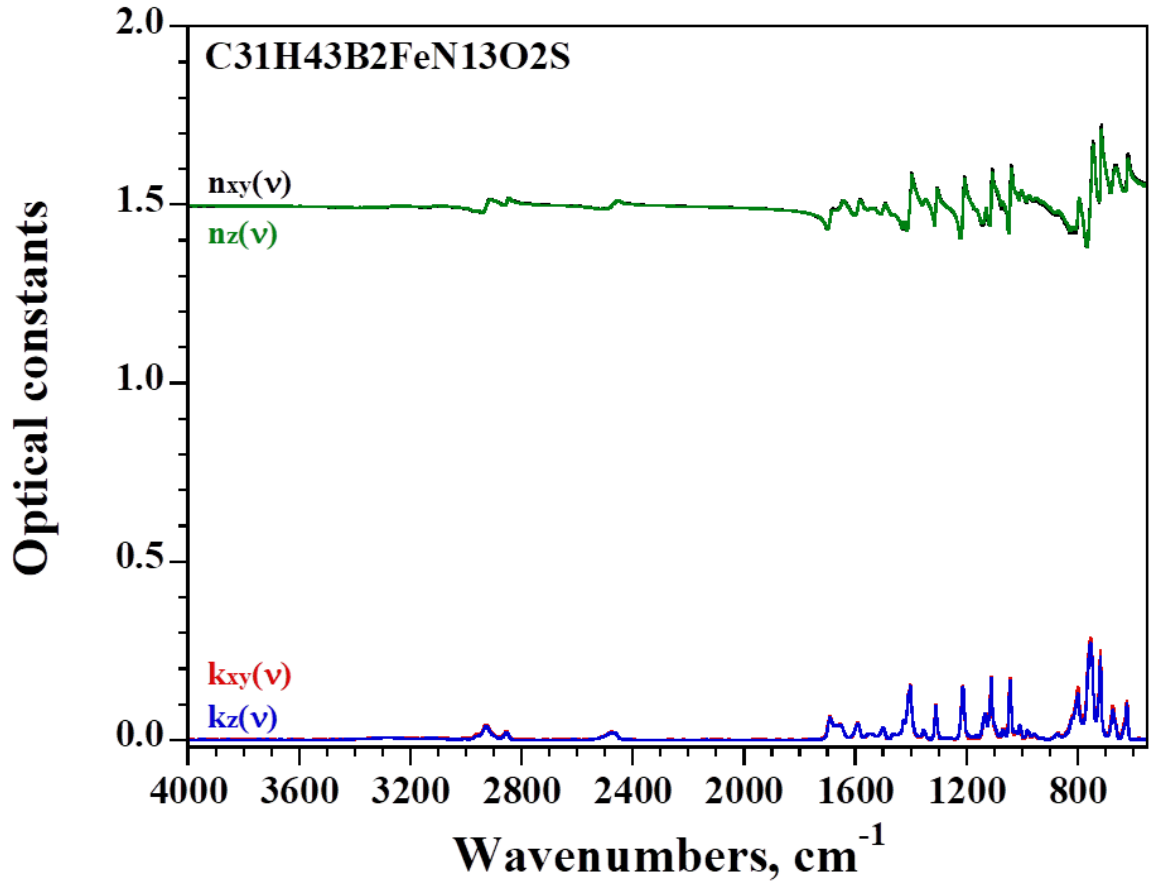

Figure S6

Cyclic voltammogram of bulk **FeTp$_2$-C11-SAc** in a solution of THF – 0.1 M NBu_4PF_6 at a scan rate of 0.05 V s^{-1}. The half-cell potential is -0.18 V with respect to the ferrocene Fc/Fc^+ redox couple.

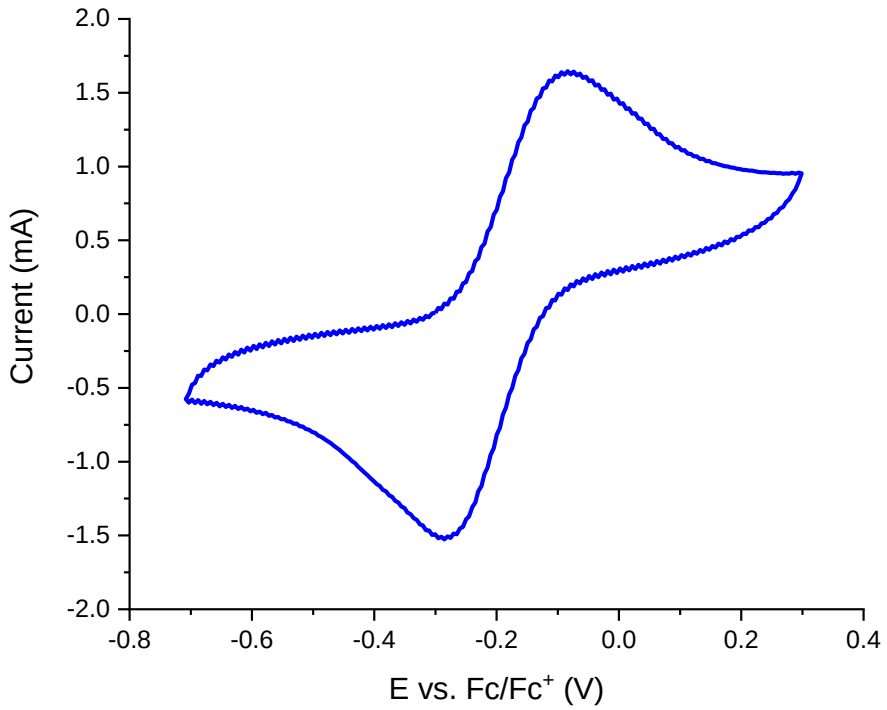

Figure S7a

X-ray absorption spectroscopy (XAS) reference spectra were measured on Au^{TS}. We assume that the spectra at 100 K are fully LS, and subtract these spectra from the corresponding spectra at 350 K in order to obtain the HS reference. The baseline was corrected by subtracting a linear and step background, as well as a contribution from gold measured on a bare Au^{TS} substrate at each temperature. The spectra were normalised by the total $L_3 + L_2$ area. The HS reference was obtained by subtracting 0.45 times the normalised LS spectrum from the normalised spectrum at 350 K.

These reference spectra are compared to the spectra obtained through ligand field multiplet calculations for octahedral HS and LS Fe(II) ($10Dq$ = 1 eV and 2.2 eV respectively) that we have previously reported.[7] The calculation energies were shifted by 1.2 and 1.9 eV to conform to experimental energies, and the spectra were normalized in the same way.

The discrepancies for the measured HS spectra are mainly at the L_3 edge 712.3 eV peak, likely because at 350 K there is not enough HS to allow for a good extraction of the HS spectral shape. For the LS spectra, deviations are seen for the feature between 717 and 721 eV, which is difficult to reproduce within the ligand field multiplet calculations as it likely originates from delocalized states over the ligand, and for the L_2 edge 727.2 eV peak. The relative variation of the L_3 and L_2 intensities due to the evolution of the branching ratio is in agreement between the experimental and calculated spectra.

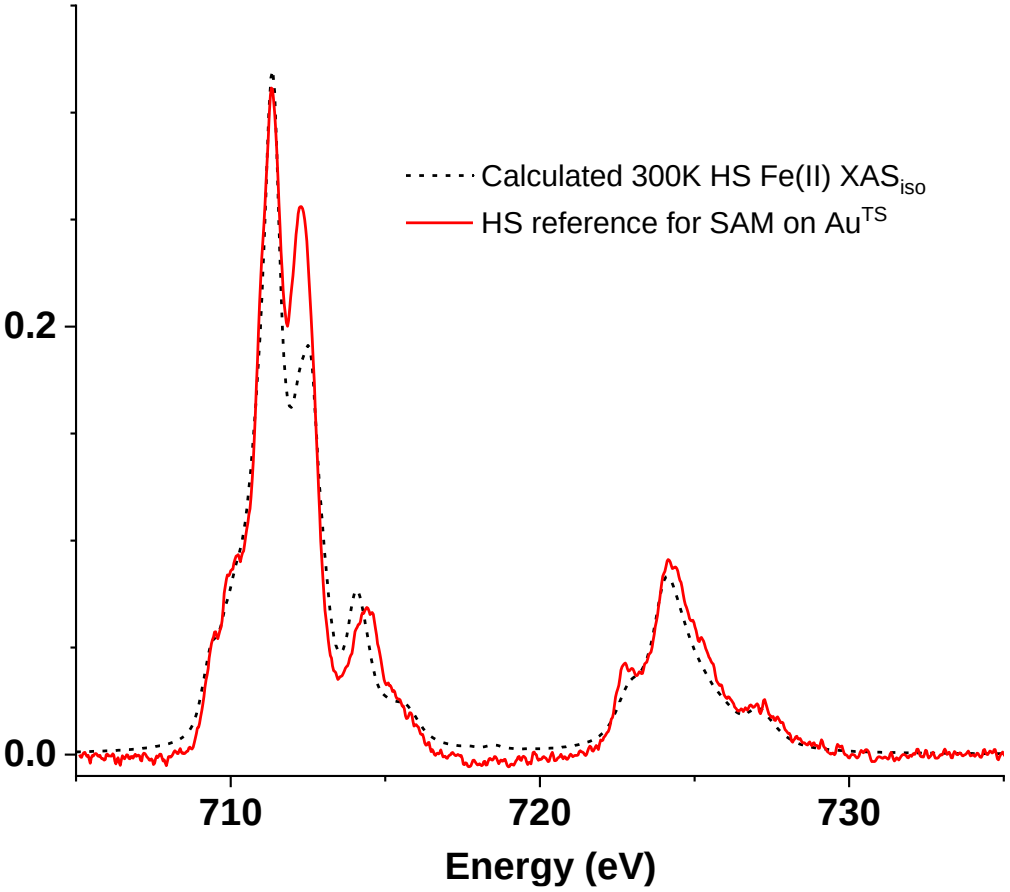
Calculated 300K HS Fe(II) XAS$_{iso}$
HS reference for SAM on Au^{TS}
0.2
0.0
710
720
730
Energy (eV)

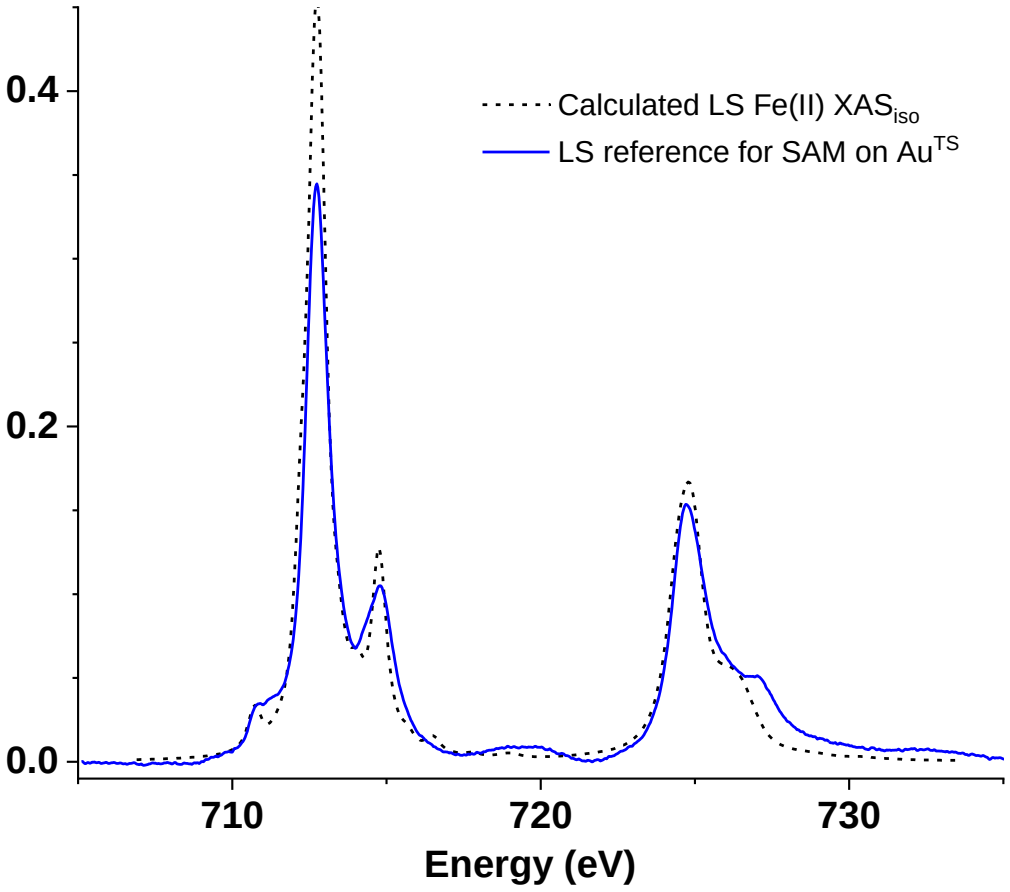
Calculated LS Fe(II) XAS$_{iso}$
LS reference for SAM on Au^{TS}
0.4
0.2
0.0
710
720
730
Energy (eV)

Figure S7b

Evolution of the Fe $L_{2,3}$ edge XAS spectra with temperature on a dropcast sample of **$FeTp_2$-C11-SAc** on copper. Linear and step backgrounds have been subtracted and the spectra normalized to have the same area. The evolution of the spectra corresponds with the evolution of the spectra of the SAM: the SCO behaviour is comparable for the bulk and SAM.

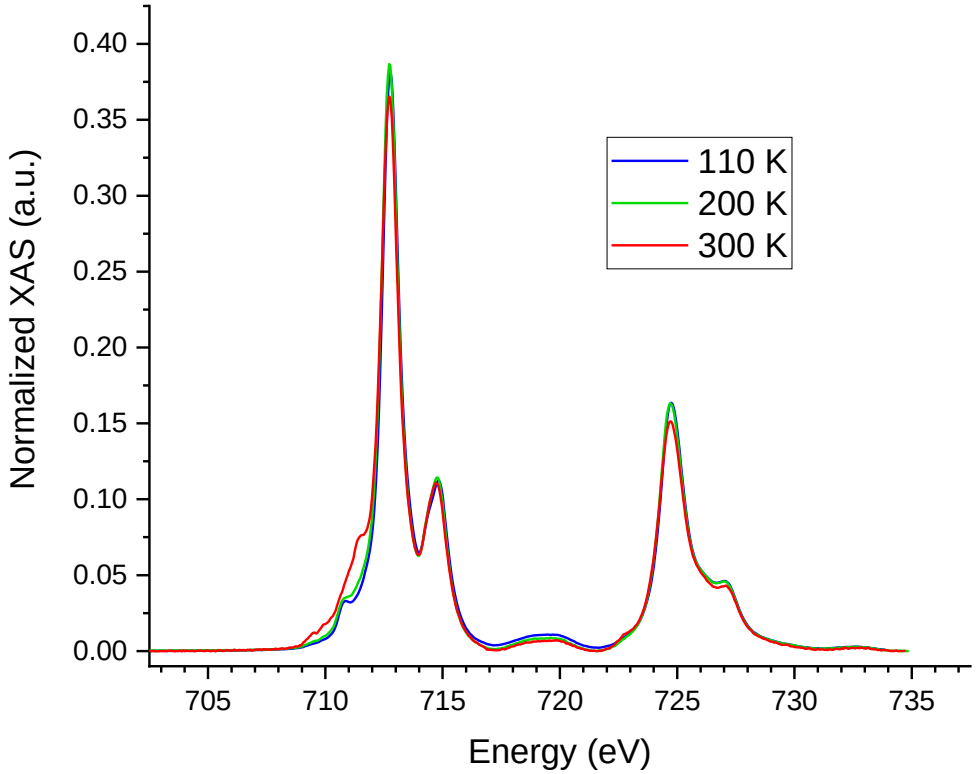

Figure S7c

Decomposition of the spectra of the SAM at each temperature into a linear combination of the LS and HS spectral shapes shown in **Figure S7a**.

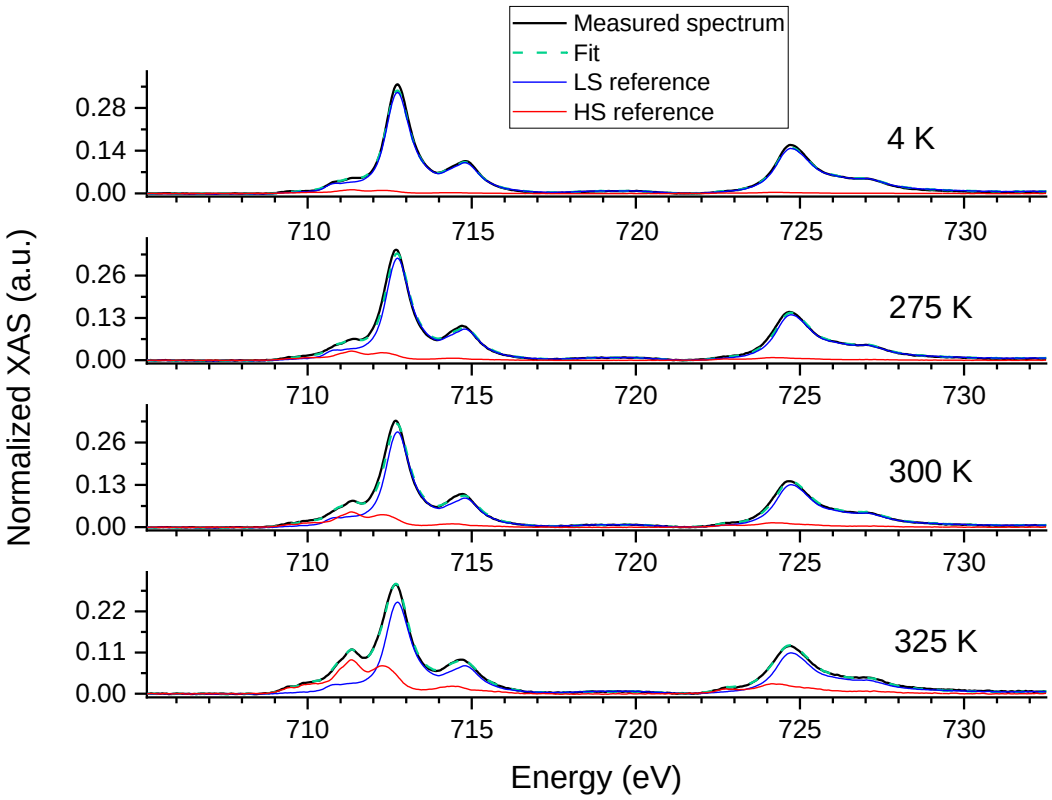

References

[1] J. J. Yeh, I. Lindau, *At. Data Nucl. Data Tables* **1985**, *32*, 1.
[2] M. J. Dignam, S. Mamiche-Afara, *Spectrochim. Acta* **1988**, *44A*, 1435.
[3] W. N. Hansen, *J. Opt. Soc. Am.* **1968**, *58*, 380.
[4] T. Buffeteau, B. Desbat, *Appl. Spectrosc.* **1989**, *43*, 1027.
[5] K. Yamamoto, H. Ishida, *Appl. Spectrosc.* **1994**, *48*, 775.
[6] E. D. Palik, *Handbook of Optical Constants of Solids*, Academic Press, New York, **1985**.
[7] B. Warner, J. C. Oberg, T. G. Gill, F. El Hallak, C. F. Hirjibehedin, M. Serri, S. Heutz, M.-A. Arrio, P. Sainctavit, M. Mannini, G. Poneti, R. Sessoli, P. Rosa, *J. Phys. Chem. Lett.* **2013**, *4*, 1546.